



Cite this: *Mol. Syst. Des. Eng.*, 2023, **8**, 323

## 4D printing of light activated shape memory polymers with organic dyes†

Matteo Gastaldi,<sup>‡a</sup> Christoph A. Spiegel,<sup>‡bc</sup> Clara Vazquez-Martel,<sup>‡bc</sup> Claudia Barolo,<sup>‡ad</sup> Ignazio Roppolo,<sup>‡\*e</sup> and Eva Blasco,<sup>‡bc</sup>

Light based 3D printing technologies, such as digital light processing (DLP), allow for the additive manufacturing of complex 3D objects at fast speeds and with high resolution. Typical printable formulations for DLP consist of (a mixture of) monomer(s), a photoinitiator and very often, an organic dye absorbing at the printing wavelength in order to improve the resolution. Herein, we exploit the use of push–pull azobenzene (azo) dyes to not only enhance printing resolution but also to enable light response (fourth-dimension) of printed shape memory polymers (SMPs) employing DLP without the necessity of adding inorganic additives. In particular, a library of azo-dyes with different substituents in ortho-position have been synthesized and added as active dyes in the printing formulation. The light activated shape memory effect is demonstrated for all the printed structures including the dyes. Among all of them, the structures containing chlorine-substituted azo dyes show the best performance. Importantly, the desired effect is achieved with only 0.1 wt% of dye in the formulation. Furthermore, we demonstrate the potential of using visible light as stimulus for spatially resolved activation of complex structures on demand.

Received 30th September 2022,  
Accepted 31st October 2022

DOI: 10.1039/d2me00201a

[rsc.li/molecular-engineering](https://rsc.li/molecular-engineering)

### Design, System, Application

In contrast to conventional approaches to induce shape changes in 4D printed geometries, light as a stimulus has the inherent advantage of temporal and spatial control. Here we have designed a shape memory polymer (SMP) ink formulation offering 4D structure fabrication at high resolution *via* digital light processing (DLP) as well as excellent light responsive properties. To achieve this, we make use of azodyes as photoresponsive moieties allowing fabrication of 4D printed structures that offer i) high printing precision as well as ii) light induced programmable shape changes, without usage of additional additives or inorganic fillers. Employing visible light irradiation, temperature was locally increased within the 4D geometry giving access to spatio-temporal activation of SMP properties. The reliability of this approach as well as the potential of visible light as stimulus was demonstrated by performing shape memory recovery processes for a range of different structures. Due to its simplicity, flexibility and reliability, we believe that the proposed system will open new possibilities in a variety of fields, such as soft robotics, actuators or smart sensing applications.

## Introduction

Since its first conceptualization in 2013, four-dimensional (4D) printing has revolutionized the worlds of additive manufacturing and design.<sup>1,2</sup> 4D printing relies on the

combination of responsive materials with additive manufacturing technologies, enabling the fabrication of smart architectures able to evolve with time in response to external stimuli. Among the external stimuli reported – solvent,<sup>3,4</sup> pH<sup>5,6</sup> or magnetic field,<sup>7,8</sup> temperature<sup>9–12</sup> is certainly the most exploited one. Common thermoresponsive polymers include hydrogels,<sup>12,13</sup> liquid crystalline elastomers<sup>14–16</sup> and shape memory polymers (SMPs).<sup>17–19</sup> The temperature activated morphism of the latter class – SMPs – is well-established and has found applications in everyday life<sup>20</sup> as medical devices, smart fabrics or packaging.<sup>21</sup>

In this context, the main approach to activate shape changes consists of heating a 3D printed structure either directly or using a thermal sink (such as water) to provide the desired temperature. Nevertheless, this strategy presents some drawbacks limiting its applicability: i) the necessity to heat the whole volume and thereby loss of any spatial control

<sup>a</sup> Department of Chemistry and NIS Interdepartmental Centre and INSTM Reference Centre, University of Torino, Via Pietro Giuria 7, 10125 Torino, Italy

<sup>b</sup> Organic Chemistry Institute, Heidelberg University, Im Neuenheimer Feld 270, 29120 Heidelberg, Germany. E-mail: [eva.blasco@oci.uni-heidelberg.de](mailto:eva.blasco@oci.uni-heidelberg.de)

<sup>c</sup> Institute for Molecular Systems Engineering and Advanced Materials, Heidelberg University, Im Neuenheimer Feld 225, 69120 Heidelberg, Germany

<sup>d</sup> ICxT Interdepartmental Center, University of Turin, Lungo Dora Siena 100, 10153 Torino, Italy

<sup>e</sup> Department of Applied Science and Technology, Politecnico di Torino, C.so Duca degli Abruzzi 24, 10129, Turin, Italy. E-mail: [ignazio.roppolo@polito.it](mailto:ignazio.roppolo@polito.it)

† Electronic supplementary information (ESI) available. See DOI: <https://doi.org/10.1039/d2me00201a>

‡ These authors contributed equally.

in terms of recovery and ii) material degradation that can take place due to applied high temperatures. Other approaches were proposed to improve localization and control of heating, such as use of current for Joule heating<sup>22</sup> or magnetic field.<sup>23</sup> Another suitable stimulus is irradiation. Light could be particularly attractive since its tunability of intensity, irradiation, irradiation time, polarization direction and wavelength allows precise spatial and temporal control.<sup>24–26</sup> One strategy to achieve light response is the incorporation of an absorber, such as an inorganic filler, which can convert the absorbed light into heat, enabling shape recovery activation. In particular, gold,<sup>27</sup> silver<sup>28</sup> and titanium<sup>29</sup> nanoparticles as well as carbon fibers,<sup>30</sup> carbon black,<sup>31</sup> graphene<sup>32</sup> and even rare earth complexes<sup>33</sup> have been successfully incorporated in SMPs enabling light-induced shape-recovery. Organic dyes, such as azobenzene derivatives (azo-dyes), are an interesting alternative to inorganic fillers, which up to now have not been fully exploited in printable SMPs. The main advantages of azo-dyes are the straightforward preparation and functionalization, which enable to fine-tune their absorption properties, as well as their photostability on demand.<sup>34</sup> The incorporation of these functional dyes in polymers, and more

specifically in liquid crystalline materials, have been extensively investigated, showing potential applications ranging from photoactuators, to photonic elements to biomedical devices.<sup>35–37</sup> Furthermore, azo-dyes are widely used in photocurable resins in light-based 3D printing techniques, such as digital light processing (DLP).<sup>9,38,39</sup> Here, the use of dyes is crucial, due to their interactions with incident curing light, improving in this way control of the polymerization reaction, enabling higher precision, higher resolution (or smaller feature sizes) and consequently allowing the fabrication of more complex structures featuring fine structural details. Recently, the use of dyes has expanded over their conventional role, using them to impart functional properties to the 3D printed components.<sup>40</sup>

Based on our prior work on the design of a functional SMP ink system for DLP 3D printing utilizing a temperature stimulus,<sup>9</sup> we attempt to expand the state-of-the-art of SMPs as printable materials and aim at the fabrication of complex 4D structures that can undergo spatially controlled shape changes. To achieve this, we employ azo-dyes as photoresponsive units to obtain 4D printed structures that offer at the same time high printing precision as well as light-induced programmable shape changes without the

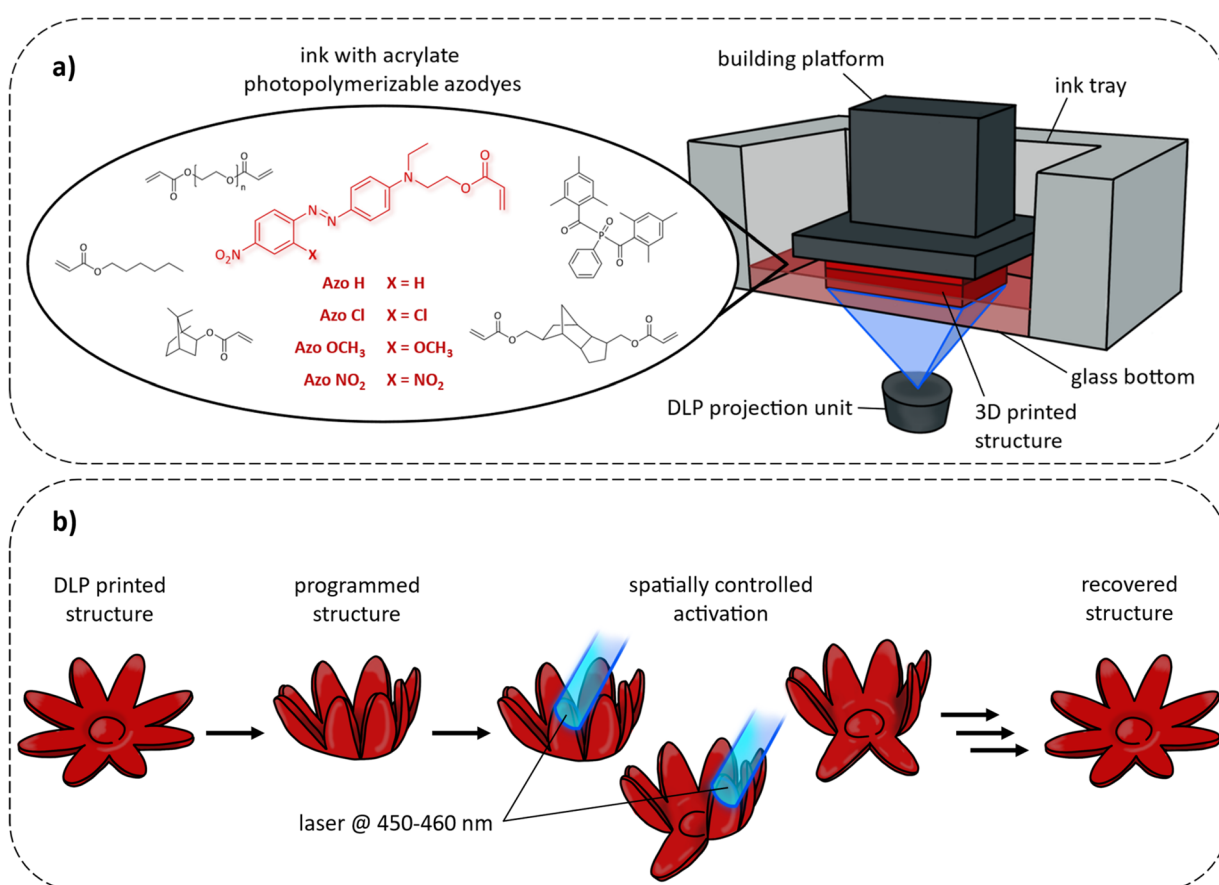


**Fig. 1** 4D printing of light activated shape memory polymers. a) Ink formulation based on acrylate monomer including photopolymerizable azo dyes and scheme of the DLP printer. b) Schematic representation of the shape memory cycle including the programming step followed by spatially controlled light induced recovery.

necessity of additional additives such as inorganic fillers. In this context, visible light irradiation will be used to locally increase the temperature and activate the SMP properties on demand (see Fig. 1).

## Results and discussion

### Identification of a functional system

Push-pull azo-dyes were selected as ideal photoresponsive units. Their role here is two-fold: i) enhancing resolution during the 3D printing process and ii) enabling light-induced shape changes of the printed structures. Thus, a library of acrylate push-pull azo-dyes (see Fig. 1) was first synthesized, introducing different functional groups in order to control the photochemical properties of the final molecules (see ESI†) through electronic or steric effects.<sup>41</sup> All the azo-dyes bear an acrylate moiety to enable covalent reaction during the 3D fabrication process and thus incorporation of the functional dyes into the polymeric network.<sup>42,43</sup> Furthermore, all azo-dyes showed absorbance in the range of 400 nm to 600 nm (see absorbance spectra in Fig. S6, ESI†), not interfering with the 3D curing wavelength of 385 nm and allowing a later shape memory recovery actuation with light in the visible range.

### 4D printing of light activated SMPs

In the next step, the synthesized azo-dyes were tested in SMP 3D printable formulations, based on a previously optimized formulation of liquid components, exhibiting good printability by DLP fabrication as well as excellent shape memory properties.<sup>9</sup> The SMP based ink is composed of isobornyl acrylate (IBA) as main component, and poly(ethylene glycol) diacrylate ( $M_n = 575 \text{ g mol}^{-1}$ , PEGDA) and tricyclo[5.2.1.0<sup>2,6</sup>] decanedimethanol diacrylate (TCMDMA) as flexible and stiff crosslinkers, hexyl acrylate

(HA), as well as phenylbis(2,4,6-trimethylbenzoyl)phosphine oxide (Irg819) as photoinitiator. The optimal concentration of azo-dye was experimentally evaluated for each sample by performing curing tests utilizing UV-LED irradiation in the range from 380 nm to 390 nm (same range as the DLP printer). In particular, we tested ink formulations with increasing amounts of azo-dye compounds AzoH, AzoCl, AzoOCH<sub>3</sub> and AzoNO<sub>2</sub> from 0.1 to 2.0 wt% and determined the time required to achieve of the resin. The results are summarized in Table S1 in the ESI.† As expected, it was observed that the higher is the azo-dye concentration, the longer time is required to achieve the photopolymerization. This is due to the competition of photon absorption between dye and photoinitiator. To not affect the efficiency of the printing process, an azo-dye concentration of 0.1 wt% was set as optimal for all inks.

Afterwards, printing parameters for each ink were carefully optimized in terms of layer thickness and curing time, aiming an efficient and precise 3D fabrication process. Conducting material tests, Jacobs working curves were obtained at  $10 \text{ mW cm}^{-2}$  for each functional ink containing AzoH, AzoCl, AzoOCH<sub>3</sub>, AzoNO<sub>2</sub> (see Fig. S7, ESI†). Critical energy values  $E_c$  were determined in the range of 3.1 to 4.3  $\text{mJ cm}^{-2}$  and values for the light penetration depth  $D_p$  were calculated in the region of 70 to 80  $\mu\text{m}$ . Setting the irradiation intensity to  $10 \text{ mW cm}^{-2}$  allowed structure fabrication with layer thicknesses of 50  $\mu\text{m}$  at short curing times between 1.5 s and 2.0 s, depending on the applied azo-dye (see Table S2, ESI†). In addition, FTIR spectra of the ink containing AzoCl and a corresponding 3D printed structure were recorded (Fig. S8, ESI†). As expected, the bands corresponding to the double bonds of the acrylate group ( $1635 \text{ cm}^{-1}$  and  $1619 \text{ cm}^{-1}$  as well as  $809 \text{ cm}^{-1}$ ) decreased, indicating their consumption during the printing process. In particular, a double bond



Fig. 2 3D printed structures using the formulation containing AzoCl: a) stripe, b) butterfly, c) flower, d) chain segment e) box, f) Pisa tower. g) Structural fidelity achieved demonstrated by the printed Pisa tower structure: heat map illustrating deviations between the 3D scanned image of the printed structure with its STL file. Scale bar = 10 mm.

conversion of around 85% was calculated (see Eqn. S2 and Fig. S9, ESI†).

The printing performance was further investigated by 3D manufacturing a range of geometries, starting from simple stripes, butterflies or flowers towards architectures featuring overhanging moieties such as the 3D box (see Fig. 2a–e for ink containing AzoCl) and concluding with highly complex structures such as the Pisa tower, allowing printability of even finest features (see Fig. 2f). In case of the Pisa tower structural fidelity of the printed geometry was further examined employing a 3D scanner. The obtained digital image was overlapped to the initial 3D model and the differences are plotted in a heat map (see Fig. 2g) showing high structural fidelity. Importantly, the resolution was further evaluated quantitatively under the microscope showing good results down to 40  $\mu\text{m}$  for all the formulations (Fig. S10, ESI†).

### Study of the opto-thermo-mechanical properties

Once the printed parameters were also optimized, we studied the opto-thermo-mechanical properties, in order to define the most effective dye to fabricate 4D devices. The activation of the shape memory process requires overcoming the glass transition temperature ( $T_g$ ) by light induced heating.<sup>44,45</sup> These values for  $T_g$  were obtained by dynamic mechanical analysis (DMA) (Fig. 3a and S11, ESI†). We employed 3D printed flat specimens ( $30 \times 10 \times 1 \text{ mm}^3$ ) from all formulations containing the different azo-dyes as well as from one without as reference (see Fig. 3a and S11 and Table S3, ESI†). An intense peak is detected at about 80  $^\circ\text{C}$ , which corresponds to the  $T_g$  of the major component (IBA monomer) in the generated network (all values are reported in Table S3†). A second weaker transition temperature centred about 30  $^\circ\text{C}$  was also observed, likely related to the aliphatic component. As expected, by comparing with the reference, no relevant modifications occur with the introduction of azo-dyes. In addition, the thermal stability of

the fabricated structures was investigated using thermogravimetry (TGA) (see Fig. S12, ESI†). It was observed, that the incorporation of azo-dyes led to a decrease of the decomposition temperature. However, all the samples are stable until 130  $^\circ\text{C}$  without showing any degradation.

To gain more insight into opto-mechanical properties of the azo-containing printed materials, DMA measurements were conducted under LED irradiation of 459 nm wavelength. In particular, the variations of the storage modulus measured while switching on and off the light were monitored (see Fig. 3b and S13, ESI†). Importantly, while the blank sample was not significantly affected, all azo-based samples exhibited a reduction in storage modulus ( $E'$ ) when irradiation by the light source was initiated due to the photothermal effect. Furthermore, this behaviour appears to be completely reversible when the light was turned off. Increasing the current of the LED power supply a faster response can be observed as well as more reduced values of storage modulus ( $E'$ ) were reached.

### Light activated shape memory effect

Shape memory tests using the 4D printed flat strips containing the different azo-dyes were performed as next step. In these experiments the printed flat strips were deformed to a temporary (bent) shape using a pre-heated water bath (80  $^\circ\text{C}$ ) and fixed using cold water at 15  $^\circ\text{C}$ . To activate the shape memory effect (recovery), the samples were irradiated using an LED (459 nm), which allows for local heating of the sample. To monitor the process, the recovery parameter  $a$  (recovered angle for bent strip) was measured as shown in Fig. S14 (ESI†) for each sample. For the samples containing azo-dyes AzoH and AzoOCH<sub>3</sub>, the time required to complete the process is about 6 and 7 minutes, while for AzoCl and AzoNO<sub>2</sub> the process was faster, taking only 4 minutes to achieve 100% of shape recovery (Fig. S15, ESI†). Considering the results obtained, AzoCl resulted as the best dye to obtain 4D structures with a good light-activated shape

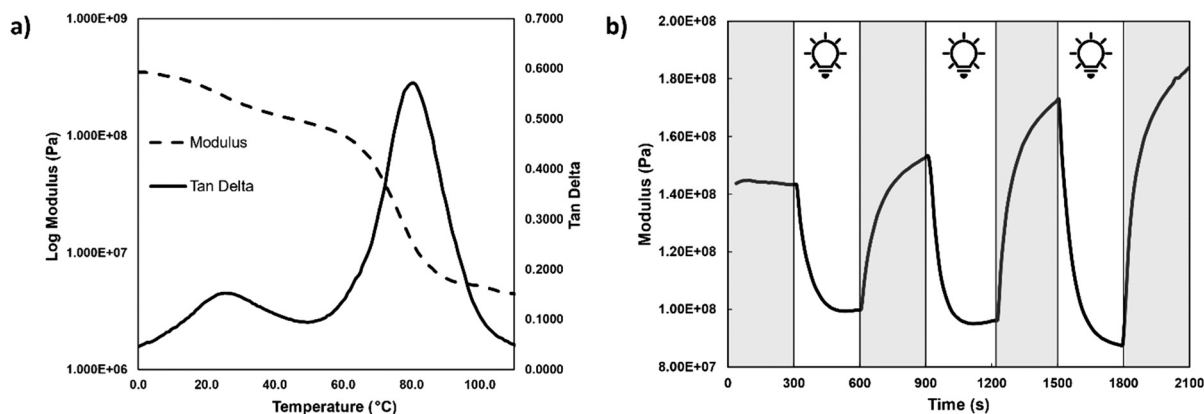
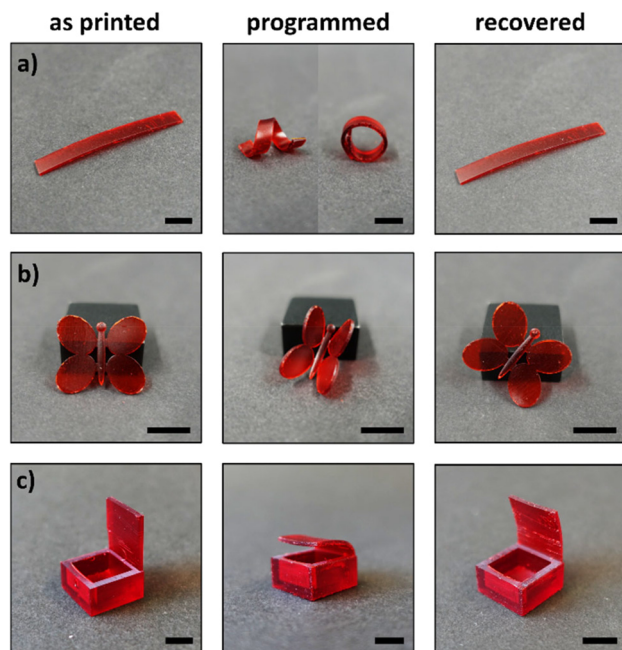


Fig. 3 Thermo-mechanical and opto-thermo-mechanical characterization. a) DMA measurement of a stripe structure fabricated with functional ink based on AzoCl. b) DMA measurement under irradiation by 459 nm LED. Timeframes without a bulb define dark state (lamp switched off), whereas timeframes marked with a bulb define irradiated state (lamp switched on).



**Fig. 4** Shape memory test of DLP-printed structures. Initial (as printed), temporary and recovered shape of a) strip, b) butterfly, c) box. Programming was performed in hot water at 95 °C, followed by fixation in cold water at 15 °C. Successive shape memory recovery was initiated by blue laser light irradiation (450–460 nm) at 567 mW cm<sup>-2</sup>. Scale bar = 10 mm.

memory effect along with its easy synthetical procedure and good printability. Thus, the ink system containing azo-dye AzoCl was selected to carry out the next shape memory experiments on more complex 3D printed shapes. After programming the different shapes, the recovery was performed using a blue laser (450–460 nm) to demonstrate the light-activated SME. The temperature reached by laser irradiation was evaluated using 3D structures containing

AzoCl and blank ink. For AzoCl structures temperatures above the higher  $T_g$  of the material and up to 125 °C were measured, despite of the low azo content, *i.e.*, 0.1 wt% (see Fig. S16 and Movie S01, ESI†), whereas blank samples show no temperature increase (see Fig. S16 and Movie S02, ESI†). In addition, FTIR spectra before and after LED irradiation resulted perfectly superimposable, indicating that no chemical changes occurred (Fig. S8†). These results are also in good agreement with TGA data and DMA data, demonstrating that the dye-induced photothermal effect did not affect material properties by photodegradation. To further demonstrate the versatility and spatial control of the system, the flat strip was programmed and fixed in several shapes – *e.g.* a circular and a helical one – and recovered back to the initial shape by laser irradiation (see Fig. 4a and Movie S03 and S04, ESI†). Moreover, we could show excellent stability of the programmed shape at room temperature within technical relevant timeframes (Fig. S17†). The programming and light induced shape recovery was also successfully evidenced utilizing complex 3D geometries such as a butterfly (see Fig. 4b and Movie S05, ESI†), a flower (see Fig. 5b and Movie S06, ESI†) and even a “smart” box that can be opened on demand (see Fig. 4c and Movie S07, ESI†).

Having demonstrated the light induced SME in different 3D printed structures, the potential of using light as stimulus was further exploited enabling spatially controlled activation and therefore, a finer manipulation of shape morphing. For visual demonstration, links and flowers were printed in the “open” state and programmed in a “closed” state. Here, the blue laser was employed to locally heat a specific region of the sample at temperatures above the  $T_g$  of the printed structure. Due to poor thermal conductivity of the polymer based material, the temperature increase is very local and the rest of the sample is barely affected allowing for a precise activation of the material in the targeted point. As a result, the recovery takes place only in the irradiated region enabling

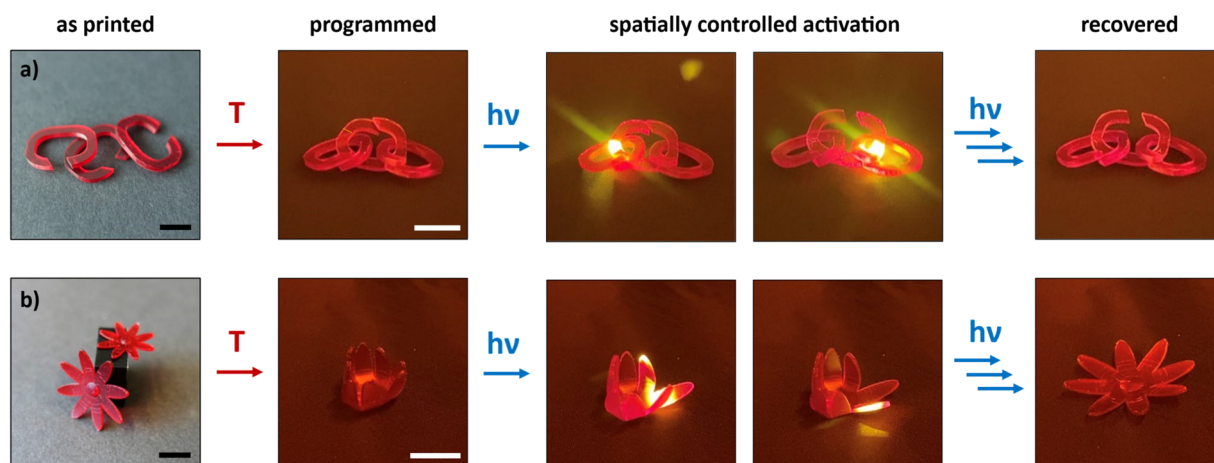


**Fig. 5** Spatially controlled recovery of the a) chain and b) flowers. Programming was performed in hot water at 95 °C, followed by fixation in cold water at 15 °C. Spatially controlled shape memory recovery was performed by irradiating the sample with blue laser light locally (450–460 nm) at 567 mW. Scale bar = 10 mm.

a partial recovery, and therefore new programmed shapes. For example, in the case of the three links, we were able to first selectively open the central segment without affecting the two outer elements (see Fig. 5a and Movie S08, ESI†), which could be opened by focusing the laser (if desired). Furthermore, this effect can be also employed to enable even more “intermediate” states. As another example, the petals of the “closed” programmed flower can be selectively opened individually on demand by focusing the laser in the intersection (see Fig. 5b, Movie S06, ESI†).

## Conclusions

In this study it has been demonstrated that push-pull azo dyes can be efficiently used to fabricate 4D printable objects. Different azo-dyes with different substituents in ortho position were synthesized and used as active dyes in a SM formulation suitable for light-activated 3D printing. All the dyes showed the ability to induce light activated shape memory behaviour. Furthermore, their presence helped the 3D printing process, increasing precision and structural fidelity. Among all the test dyes, the one modified with chlorine offered the best performance in terms of percentage and speed of recovery of the initial shape. Thermal tests performed on complex shape 3D printed objects evidenced a rapid increase of temperature induced by the presence of azo compounds. Furthermore, this temperature increase results localized in the irradiated area allowing for shape recovery with excellent spatial control. This was exploited in several 4D printed demonstrators, which showed light-induced spatial and time control over the shape memory properties. SME behaviour resulted also to be repeatable, indicating that despite temperature increase, dyes do not degrade, allowing to maintain the light-responsive property over time. Noteworthy, the light-controlled activation of shape memory behaviour is based on a component which is added at only 0.1 wt% of the ingredients. These findings can find multiple applications in soft robotics, advanced sensors, and biological studies.

## Author contributions

M. G., C. A. S. and C. V. M.: data curation, methodology, investigation, software, formal analysis, visualization, writing – original draft. C. B., I. R. and E. B.: conceptualization, methodology, formal analysis, funding acquisition, resources, project administration, supervision, writing – review & editing.

## Conflicts of interest

There are no conflicts to declare.

## Acknowledgements

E. B. acknowledges the funding from the Deutsche Forschungsgemeinschaft (DFG, German Research

Foundation) via the project BL-1604/2-1 and the Excellence Cluster “3D Matter Made to Order” (EXC-2082/1-390761711) and the Carl Zeiss Foundation through the “Carl-Zeiss-Foundation-Focus@HEiKA”. C. V. M. acknowledges the Fonds der Chemischen Industrie for the support during her PhD studies. The authors thank P. Kiefer (Karlsruhe Institute of Technology) for his help with the light microscope measurements. The authors also want to thank Y. Rahman (Karlsruhe Institute of Technology) for the fruitful discussions.

## Notes and references

- 1 P. Fu, H. Li, J. Gong, Z. Fan, A. T. Smith, K. Shen, T. O. Khalafallah, H. Huang, X. Qian, J. R. McCutcheon and L. Sun, *Prog. Polym. Sci.*, 2022, **126**, 101506.
- 2 X. Kuang, D. J. Roach, J. Wu, C. M. Hamel, Z. Ding, T. Wang, M. L. Dunn and H. J. Qi, *Adv. Funct. Mater.*, 2019, **29**, 1805290.
- 3 A. S. Gladman, E. A. Matsumoto, R. G. Nuzzo, L. Mahadevan and J. A. Lewis, *Nat. Mater.*, 2016, **15**, 413.
- 4 Z. Zhao, X. Kuang, C. Yuan, H. J. Qi and D. Fang, *ACS Appl. Mater. Interfaces*, 2018, **10**, 19932.
- 5 Y. Hu, Z. Wang, D. Jin, C. Zhang, R. Sun, Z. Li, K. Hu, J. Ni, Z. Cai, D. Pan, X. Wang, W. Zhu, J. Li, D. Wu, L. Zhang and J. Chu, *Adv. Funct. Mater.*, 2020, **30**, 1907377.
- 6 C. Garcia, A. Gallardo, D. López, C. Elvira, A. Azzahti, E. Lopez-Martinez, A. L. Cortajarena, C. M. González-Henríquez, M. A. Sarabia-Vallejos and J. Rodríguez-Hernández, *ACS Appl. Bio Mater.*, 2018, **1**, 1337.
- 7 S. Roh, L. B. Okello, N. Golbasi, J. P. Hankwitz, J. A.-C. Liu, J. B. Tracy and O. D. Velev, *Adv. Mater. Technol.*, 2019, **4**, 1800528.
- 8 Y. Zhang, Q. Wang, S. Yi, Z. Lin, C. Wang, Z. Chen and L. Jiang, *ACS Appl. Mater. Interfaces*, 2021, **13**, 4174.
- 9 C. A. Spiegel, M. Hackner, V. P. Bothe, J. P. Spatz and E. Blasco, *Adv. Funct. Mater.*, 2022, 2110580.
- 10 K. Liu, Y. Zhang, H. Cao, H. Liu, Y. Geng, W. Yuan, J. Zhou, Z. L. Wu, G. Shan, Y. Bao, Q. Zhao, T. Xie and P. Pan, *Adv. Mater.*, 2020, **32**, 2001693.
- 11 M. Hua, D. Wu, S. Wu, Y. Ma, Y. Alsaïd and X. He, *ACS Appl. Mater. Interfaces*, 2021, **13**, 12689.
- 12 M. Hippler, E. Blasco, J. Qu, M. Tanaka, C. Barner-Kowollik, M. Wegener and M. Bastmeyer, *Nat. Commun.*, 2019, **10**, 232.
- 13 M. Champeau, D. Alves Heinze, T. Nunes Viana, E. Rodrigues de Souza, A. C. Chinellato and S. Titotto, *Adv. Funct. Mater.*, 2020, **30**, 1910606.
- 14 Z. Guan, L. Wang and J. Bae, *Mater. Horiz.*, 2022, **9**, 1825.
- 15 M. del Pozo, J. A. H. P. Sol, A. P. H. J. Schenning and M. G. Debije, *Adv. Mater.*, 2022, **34**, 2104390.
- 16 A. Münchinger, V. Hahn, D. Beutel, S. Woska, J. Monti, C. Rockstuhl, E. Blasco and M. Wegener, *Adv. Mater. Technol.*, 2022, **7**, 2100944.
- 17 J. Zhang, Z. Yin, L. Ren, Q. Liu, L. Ren, X. Yang and X. Zhou, *Adv. Mater. Technol.*, 2022, 2101568.

- 18 Q. Ge, A. H. Sakhaei, H. Lee, C. K. Dunn, N. X. Fang and M. L. Dunn, *Sci. Rep.*, 2016, **6**, 31110.
- 19 B. Zhang, H. Li, J. Cheng, H. Ye, A. H. Sakhaei, C. Yuan, P. Rao, Y.-F. Zhang, Z. Chen, R. Wang, X. He, J. Liu, R. Xiao, S. Qu and Q. Ge, *Adv. Mater.*, 2021, **33**, 2101298.
- 20 M. Behl and A. Lendlein, *Mater. Today*, 2007, **10**, 20.
- 21 Y. Xia, Y. He, F. Zhang, Y. Liu and J. Leng, *Adv. Mater.*, 2021, **33**, 2000713.
- 22 A. Cortés, A. Cosola, M. Sangermano, M. Campo, S. González Prolongo, C. F. Pirri, A. Jiménez-Suárez and A. Chiappone, *Adv. Funct. Mater.*, 2021, **31**, 2106774.
- 23 F. Zhang, L. Wang, Z. Zheng, Y. Liu and J. Leng, *Composites, Part A*, 2019, **125**, 105571.
- 24 M. Herath, J. Epaarachchi, M. Islam, L. Fang and J. Leng, *Eur. Polym. J.*, 2020, **136**, 109912.
- 25 E. Pantuso, G. D. Filpo and F. P. Nicoletta, *Adv. Opt. Mater.*, 2019, **7**, 190025.
- 26 R. Klajn, *Chem. Soc. Rev.*, 2014, **43**, 148.
- 27 H. Zhang and Y. Zhao, *ACS Appl. Mater. Interfaces*, 2013, **5**, 13069.
- 28 N. Yenpech, V. Intasanta and S. Chirachanchai, *Polymer*, 2019, **182**, 121792.
- 29 S. Ishii, K. Uto, E. Niiyama, M. Ebara and T. Nagao, *ACS Appl. Mater. Interfaces*, 2016, **8**, 5634.
- 30 H. M. C. M. Herath, J. A. Epaarachchi, M. M. Islam, W. Al-Azzawi, J. Leng and F. Zhang, *Compos. Sci. Technol.*, 2018, **167**, 206.
- 31 Y. Liu, G. Zhu, W. Liu, H. Liu, Y. Huo, T. Ren and X. Hou, *Smart Mater. Struct.*, 2018, **27**, 095008.
- 32 J. Loomis, X. Fan, F. Khosravi, P. Xu, M. Fletcher, R. W. Cohn and B. Panchapakesan, *Sci. Rep.*, 2013, **3**, 1900.
- 33 L. Fang, S. Chen, T. Fang, J. Fang, C. Lu and Z. Xu, *Compos. Sci. Technol.*, 2017, **138**, 106.
- 34 P. Weis, W. Tian and S. Wu, *Chem. – Eur. J.*, 2018, **24**, 6494.
- 35 H. Zeng, P. Wasylczyk, C. Parmeggiani, D. Martella, M. Burrelli and D. S. Wiersma, *Adv. Mater.*, 2015, **27**, 3883.
- 36 D. Martella, S. Nocentini, D. Nuzhdin, C. Parmeggiani and D. S. Wiersma, *Adv. Mater.*, 2017, **29**, 1704047.
- 37 M. del Pozo, J. A. H. P. Sol, A. P. H. J. Schenning and M. G. Debije, *Adv. Mater.*, 2022, **34**, 2104390.
- 38 S. Deng, J. Wu, M. D. Dickey, Q. Zhao and T. Xie, *Adv. Mater.*, 2019, **31**, 1903970.
- 39 D. Ahn, L. M. Stevens, K. Zhou and Z. A. Page, *ACS Cent. Sci.*, 2020, **6**, 1555.
- 40 M. Gastaldi, F. Cardano, M. Zanetti, G. Viscardi, C. Barolo, S. Bordiga, S. Magdassi, A. Fin and I. Roppolo, *ACS Mater. Lett.*, 2021, **3**, 1.
- 41 J. V. Accardo and J. A. Kalow, *Chem. Sci.*, 2018, **9**, 5987.
- 42 M. Gillono, I. Roppolo, F. Frascella, L. Scaltrito, C. F. Pirri and A. F. Chiappone, *Appl. Mater. Today*, 2020, **18**, 100470.
- 43 I. Roppolo, A. Chiappone, A. Angelini, S. Stassi, F. Frascella, C. F. Pirri, C. Ricciardi and E. Descrovi, *Mater. Horiz.*, 2017, **4**, 396.
- 44 R. Suriano, R. Bernasconi, L. Magagnin and M. Levi, *J. Electrochem. Soc.*, 2019, **166**, B3274.
- 45 A. P. Piedade, *J. Funct. Biomater.*, 2019, **10**, 9.